A Sensitivity Quantification Approach to Significance Analysis of Thrusters in Dynamic Positioning Operations

Chunlin Wang[a], Guoyuan Li[a,*], Robert Skulstad[a], Xu Cheng[b], Ottar Osen[c] and Houxiang Zhang[a]

[a]Department of Ocean Operations and Civil Engineering, Norwegian University of Science and Technology, 6009 Ålesund, Norway
[b]Department of Manufacturing and Civil Engineering, Norwegian University of Science and Technology, 2815 Gjøvik, Norway
[c]Department of ICT and Natural Sciences, Norwegian University of Science and Technology, 6009 Ålesund, Norway

ARTICLE INFO

Keywords:
Dynamic positioning capability
Sensitivity analysis
Statistical analysis
Thruster failures

ABSTRACT

The safety of offshore operations is highly dependent on the dynamic positioning (DP) capability of a vessel. Meanwhile, DP capability comes down to the ability of the thrust generated by thrusters to counteract environmental forces. Therefore, it is significant to investigate which thrusters are important to the position-keeping ability of vessels. However, complex environmental factors make the investigation of thrusters' importance more complicated. Hence, this paper proposes a new method to identify the influence of each thruster on vessel's station-keeping capability in different sea states. The station-keeping capability is quantified by a defined synthesized positioning ability criterion comprised by vessel position, heading angle, and consumed power. Through the comparison of different machine learning approaches, support vector machine (SVM) is used for building a surrogate model between DP capability and thrusters. In order to determine the most sensitive thruster in the whole process of vessel operation, an improved sensitivity analysis (SA) called 'PAWN' is employed along with statistical analysis to evaluate the significance of thrusters from different perspectives. Seventeen cases are investigated with respect to different thruster failures in various sea states. The results show the proposed method is able to identify the significance of each thruster in different scenarios.

1. Introduction

As the exploration and exploitation of marine resources such as oil and gas, renewable energy and other minerals, marine operations are becoming more and more frequent in recent years. Due to the influence of environmental disturbances, it represents significant safety and integrity challenges that shall threaten the offshore operations. For the sake of safe offshore operations, vessels with dynamic positioning (DP) system are playing a critical role. They can automatically maintain the desired position. In order to ensure that a loss of position shall not occur even after a worst-case failure in all components, DP 2 and DP 3 are designed with redundant power systems in which 20% of electrically generated power shall be reserved [1]. The high position-keeping ability of DP 2 and DP 3 enables them to work in various offshore operations. Their wide applications have drawn great attention from stakeholders. Many researchers devoted to optimizing control parameters, improving controller performance, and detecting thruster failure [2, 3, 4]. However, few of them investigated the interior relation between thrusters and the vessel's DP capability. Hence, it is of great potential to analyze the interaction among thrusters and environmental factors for on-board support of the vessel's DP capabilities improvement.

In order to test the operational safety of DP vessels, a digital twin is introduced and widely used in the service of designing and evaluating system performance, safety, and structural integrity. It is a digital model that integrates data from varying sources, and can simulate all operations in the real asset while saving time and money. The digital twin has been successfully applied in a simulation of DP operations as well as the assessment of DP capability [5]. As all DP vessels carry a risk of loss of position, which has detrimental effects on personnel, the environment and equipment [6], they have a high requirement of DP capability. For the assessment of DP capability of a vessel, thruster's failures are also seen as the first concern in most of assessing guidelines [7]. It makes sense to use digital simulation platform for investigating whether vessels can provide sufficient forces using the rest of thrusters to counteract against environmental loads when a certain thruster failure occurs such as a tunnel thruster failure or a main thruster failure.

To date, there have been many attempts to analyze thruster failure in marine operations. Xu et al. developed a novel synthesized criterion to analyze the positioning performance of DP vessels. Various thruster failures were considered in the research [8]. Benetazzo et al. utilized a parity space approach and a Luenberger observer to gain the residuals. Next, the cumulative sum algorithm was applied on these residuals to detect and isolate thruster failures [9]. Sheng et al. developed a program to investigate the DP capability of semi-submersible vessels under the case of thruster failure [10]. This research contributed to demonstrating the safety of the DP system and provided adequate guidance to the thrust system's design. Han et al. used a deep Convolutional Neural Network method to detect the potential thruster failure [4]. This data-driven method had a good performance to detect and isolate thruster failure without any vessel-dependent models. However, the relation between DP capability and thruster failures is not investigated further

*Corresponding author
guoyuan.li@ntnu.no (G. Li)
ORCID(s): 0000-0001-7511-2910 (C. Wang); 0000-0001-7553-0899 (G. Li)

for papers as mentioned above. Xu et al. proposed a method using sensitivity analysis (SA) to investigate the influence of thrusters on positioning capability [11]. However, the paper adopted local SA which can not reflect the characteristics of vessel sea-keeping ability in whole input space. Cheng et al. used global SA method to analyze thrusters' importance to ship heading [12]. Nevertheless different thruster failure cases were not considered in their study. In a word, there are few researches to carry out a comprehensive analysis of how much contribution thrusters make to DP capability in the case of various thruster failures and different sea states.

This paper proposes a novel methodology to analyze the significance of each thruster on DP capability. It could not only provide onboard support for improving DP capability, but also give guidance for power system design as well as thrusters' maintenance with the help of statistical analysis and SA. The predominant contributions are as follows: 1) positioning capability is quantified by a designed synthesized criterion made up of ship position, heading angle, and consumed power; 2) machine learning (ML) and a modified PAWN are combined to quantify the significance of each thruster; 3) this method is applied to analyze the importance of each thruster during DP operation in different failure conditions and environmental load scenarios.

The rest of this paper is structured as follows: the next section describes related works on DP capability assessment and SA. Section 3 details the procedure of obtaining significance of thrusters from data generation, data preprocessing, an optimal ML selection to significance analysis. Section 4 compares the performance of ML based on the benchmark function, and tests the ability of the proposed method to analyze the importance of thrusters using professional simulator in a variety of scenarios. Section 5 is conclusion.

2. Related works

2.1. Dynamic positioning capability assessment

Some offshore operations, like oil production, pipe laying, and drilling, deeply rely on DP capability to maintain vessel position or heading within an accepted criterion. Traditionally, dynamic positioning capability (DPCap) analysis is performed based on industrial standards, such as 'IMCA M140', 'DNV GL ERN', and 'ABS skp' [13]. DPCap studies test whether the vessel has favorable actuator capacity to counteract environmental loads while keeping a constant position [14]. However, they have limited ability to provide other relevant and desired information. A significant shortcoming of the quasi-static DPCap analysis is the inability to consider the transient conditions during a failure and recovery after the failure [15].

These deficiencies call for the development of next-level DP capability analysis. Dynamic capability (DynCap) was proposed to determine the station-keeping capability of a vessel using systematic time-domain simulations. It employs a complete six-degree of freedom (DOF) vessel model. This model includes dynamic environmental loads, a complete propulsion system with thrust losses and so on [15]. One of the advantages of the DynCap analysis, compared to traditional DPCap, is that the limiting environment can be computed by applying a set of user-defined acceptance criteria. The position and heading excursion are set to allow a wide or narrow footprint. The 'DNVGL-ST-0111' standard introduced detailed requirements, principles and acceptance criteria [1]. It also provides complete analysis methods for the three DP capability levels.

Many researchers have been working on DP capability analysis for decades. Pivano et al. performed full-scale trials using the DynCap method to validate a vessel's station-keeping capability [13]. Different comparisons were made by statistics of time-domain data with various environmental loads.

Xu et al. investigated positioning performances for DP vessels considering thruster failure modes by a synthesized criterion [8]. The criterion is used to quantify the positioning ability by integrating positioning accuracy and consumed power. However, these criteria can not fully represent the DP capability from the perspective of statistics.

In this study, positioning capability refers to how well the DP vessel is positioned, instead of the extremity of the environmental conditions the vessel can counteract, as underlined by [11]. Based on prior studies and our SA method [16], positioning capability is quantified by time-series ship parameters such as ship position, heading, and consumed power. Some aforementioned statistics of time-domain data to analyze the DP capability of offshore vessels were accepted and adopted.

2.2. Sensitivity analysis

SA is a powerful tool to identify how much the variation of model output can be apportioned to inputs [17]. SA, in general, is made up of variance-based and density-based methods.

Variance-based methods includes Sobol [18], the Fourier Amplitude Sensitivity Test (FAST) [19], and the Extend-FAST (EFAST) [20] and so on. A well-known advantage of variance-based methods is their ability to quantify the individual parameter contribution and the contribution resulting from parameter interactions [21]. However, variance-based methods do not completely represent the output uncertainty when the model output is highly skewed [22].

To overcome this drawback, a new method called moment-independent global SA method—also known as density-based method, was proposed, which includes an Entropy-based sensitivity measure [23] and the δ-sensitivity method [24]. However, optimal bandwidth selection has a high computational cost. Hence, the development of these methods has been limited. Francesca et al. came up with a novel SA method called 'PAWN' that characterizes the output distribution by its cumulative distribution function (CDF) instead of probability distribution function (PDF) [17]. One advantage of PAWN is that it hugely reduces computational cost because there is no need to compute unknown parameters for the approximation of empirical CDF. Another

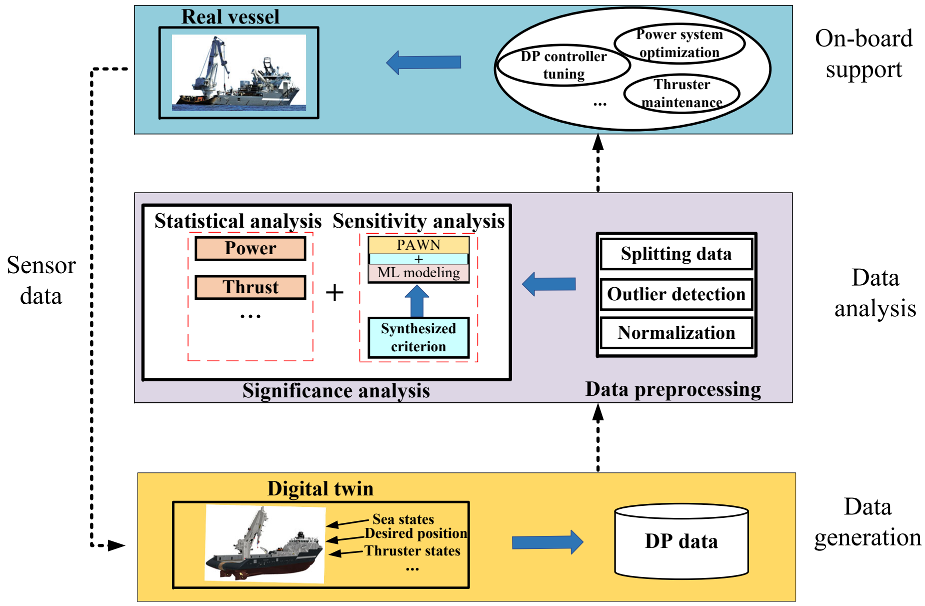

Figure 1: The system structure of significance analysis of thrusters in DP operations.

advantage is that sensitivity indices can be easily obtained, by considering either entire range of variation of the model output or a sub-range.

SA is widely applied for maritime applications with different purposes. Li et al. applied a derivative-based SA method to simplify a neural network (NN) model so as to predict ship motion [25]. Zhang et al. adopted a sum of square derivatives to choose inputs for the nonlinear auto aggressive model in order to create a compact ship motion model [26]. Mizythras et al. proposed an SA to determine parameters that have impacts on vessel propulsion and maneuverability [27].

In this study, based on our previous experience [16], the PAWN method is adopted to conduct an SA of thrusters. In addition, we make some modifications and improvements according to features of DP data.

3. System structure

This section outlines the procedure of significance analysis of thrusters in DP operations. The workflow consists of three parts as shown in Fig. 1. The first part generates raw simulated DP data by DP simulator which is considered as a digital twin of a real vessel. Users are able to change inputs to the simulator, such as sea states, desired position, and thruster states, to simulate different scenarios to obtain several data sets. After the behavior of vessel changes over time, new raw sensor data are generated and come into the digital platform for further modeling and simulation. The second part is data analysis that is made of data preprocessing and significance analysis. Outcomes of analysis are used to offer on-board support of real vessel's operations as well as system optimization.

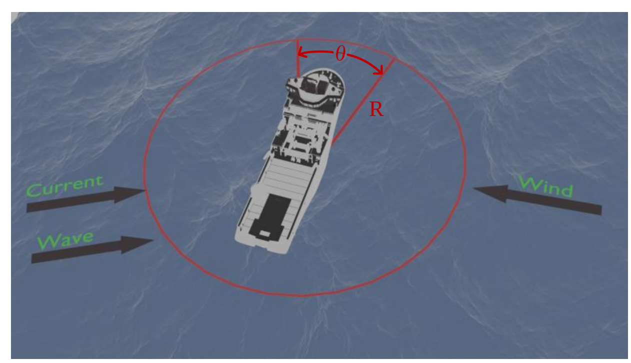

Figure 2: DP operations of a vessel at sea.

3.1. DP data generation

In the study, the DP data are generated from a professional simulator in the Offshore Simulator Centre — the world's most advanced provider of simulators for demanding marine operations[1]. Fig. 2 illustrates the simulator conducting DP operation under the impact of environmental disturbances. Its position is limited within a red circle whose diameter is denoted as R. The limit of heading is restricted by red sector whose angle is represented as θ. Fig. 3 shows the environmental effects on the ship. Wind with an attack angle of α can be changed in the simulation. Current and wave coming from other directions are fixed in the study. In Fig. 3, the Earth-fixed reference frame is denoted as (X_E, Y_E). The body-fixed reference frame (X,Y) is fixed on the body of the vessel. Its origin is the vessel's center of gravity. The DP vessel is equipped with six thrusters including four tunnel thrusters (Thruster 1-4) and two main thrusters (Thruster 5 and 6). In the simulator, sea state, thruster state, and the

[1] https://osc.no/

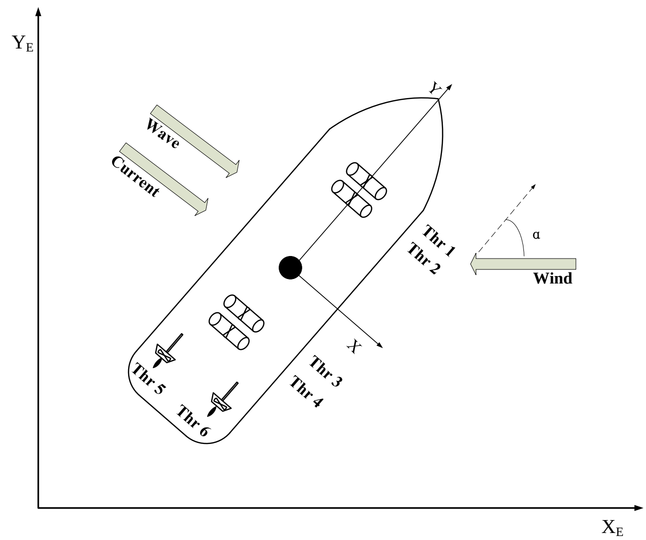

Figure 3: The thruster configuration of DP vessel.

desired position are all adjustable.

In this paper, two different sea states are investigated as shown in Table 1. The desired position is set to (0,0). Thruster states involve various thruster failure modes. Based on our experiment design, after the corresponding thrusters are shut off, the rest of thrusters are used for actuating vessel to generate several groups of time-domain DP data. For each sea state, experiments are performed on different thruster failure modes. Then ship position and heading are obtained after each experiment, and the other ship state parameters such as thruster arguments are obtained as shown in Table 3. These time series data are raw DP data. They will be processed in the following step.

Table 1
Sea states

Beaufort description	Wind velocity (m/s)	Wave height (m)	Wave period (s)	Current speed (m/s)
Fresh breeze	7.90	1.30	6.50	0.75
Strong breeze	13.80	3.10	8.50	0.75

3.2. Data preprocessing

Data preprocessing makes it possible to ensure efficiency and accuracy for computation of the computed PAWN sensitivity indices. It requires three substeps that are splitting data, denoising, and normalization. This experiment was set as a ship that was intact at the beginning but in failure mode by the end. The whole experiment produced a lot of time-series DP data related to various combinations of thruster failure modes and sea states. These data are full of anomalies resulting from noise, which would threaten the accuracy of SA. In this paper, Isolation Forest (iForest) was applied for data cleaning. The iForest is an algorithm that uses a tree structure to isolate instances [28]. It can (i) achieve a low linear time-complexity and a small memory-requirement, and (ii) deal with the effects of swamping and masking effectively. iForest detection is a two-stage process. The first stage uses the given training data to build an isolation tree. The second one computes an average path length of each instance through isolation trees.

Let $X = [x_1, x_2, ..., x_m] \subseteq \mathbb{R}^{m\times d}$ be a sample set of m instances with d-variate distribution. Firstly, iForest is constructed by the proposed algorithm in [29]. Secondly, path length $h(x)$ of each instance is computed by counting the number of edges from the root node to a leaf node in an iTree. Next, Eq. (1) is used to gain $c(\psi)$ that is the average of $h(x)$ given ψ.

$$c(\psi) = \begin{cases} 2H(\psi-1) - 2(\psi-1)/m & \psi > 2, \\ 1 & \psi = 2, \\ 0 & otherwise. \end{cases} \tag{1}$$

where ψ is the subsampling size during the stage of building an iForest; H(i) is the harmonic number which can be estimated by Euler's constant (ln(i)+0.57721). Finally, Eq. (2) is used to calculate the score of every instance:

$$s(x,\psi) = 2^{\frac{E(h(x))}{c(\psi)}} \tag{2}$$

where $E(h(x))$ is the expectation of $h(x)$ from the collection of iTrees. If s is close to 1, then the instance is seen as an anomaly and removed from the data set.

After data cleaning, these data need to be normalized in the range of [0, 1] by Eq. (3) for the purpose of formulating a synthesized criterion.

$$\tilde{x}_i = \frac{\hat{x}_i - min(\hat{X})}{max(\hat{X}) - min(\hat{X})} \quad i = 1 \ldots l \tag{3}$$

where $\hat{X} = [\hat{x_1}, \hat{x_2}, \ldots, \hat{x_l}] \subseteq \mathbb{R}^{l\times d}$. Therein, l is smaller than m because some abnormal instances are removed. After the procedure of data pre-processing, the processed data will be used to create a synthesized criterion to construct a surrogate model.

3.3. Significance analysis

Significance analysis is the last step to identify the significance of thrusters. It is comprised of statistical analysis and SA. These two methods can analyze the significance of thrusters from different respects. Meanwhile, the integration of both methods can provide guidance for power allocation, DP system optimization. Statistical analysis focuses on statistical features of DP data by virtue of mean, maximum value, variance and PDF [13]. As a supplementary instruction for SA, it is able to show the variation of each of data attributes intuitively. SA is capable of quantifying the contribution of each thruster to DP capability. It is comprised of three portions: 1) proposing a synthesized criteria to quantify DP capability; 2) selecting an optimal ML method to build a surrogate model; 3) using PAWN to compute sensitivity indices.

3.3.1. Synthesized criterion

To investigate the significance of every thruster on positioning capability in different sea states and failure modes, a synthesized criterion that quantifies the positioning performance needs to be defined. This criterion is used to evaluate how well the ship is positioned. According to the DP capability level in 'DNVGL-ST-0111' standard, assessment of station-keeping capability is mainly based on statistics of the position deviation and heading deviation. Therefore, position and heading should be integrated into the synthesized criterion. In addition, for ensuring the safety and accuracy of DP operations, the DP vessel has a higher power requirement than other conventional vessels [8]. Therefore, power consumption is also taken into consideration in this criterion. As a result, we create a synthesized criterion by Eq. (4) to lump the above-mentioned ship parameters together, with extra modification to make it adapt to the SA method.

$$\begin{cases} V = \omega_1 \times D + \omega_2 \times A + \omega_3 \times P \\ \omega_1 + \omega_2 + \omega_3 = 1 \\ Cri = -ln(V) \qquad\qquad V > 0. \end{cases} \tag{4}$$

where ω_1, ω_2, and ω_3 are weighting factors within [0,1]; D is position deviation computed by the distance between current and original position; A denotes the heading angle variation; P represents total power consumed by thrusters; Cri is the synthesized criterion computed by the inverse of the monotone increasing function 'ln'. The larger V is, the worse the positioning capability (Cri). Compared to the exponential function in the interval [0,1], the minus of 'ln' function can amplify the value of V to better reflect the distinction of positioning capability [30]. Cri will be used as the model output when ML trains a surrogate model between thrusters' parameters and DP capability.

3.3.2. Sensitivity analysis

A modified PAWN is adopted as an SA method to quantify the influence of thrusters to positioning capability. Compared with traditional method, it is able to overcome the issue of being hard to define three parameters, i.e., the number of unconditional input samples (N_u), the number of conditional input samples (N_c), and the number of conditional points (n) [31].

Let $\langle \tilde{X}, Y \rangle$ be a generic sample where $\tilde{X}$ is the processed input samples; Y denotes the value of quantifying DP capability. It is handled by splitting the range of input factor $\tilde{x_i}$ into n equal subintervals I_k. The PAWN indices approximation is shown as follows:

$$\begin{cases} \hat{S}_i = \underset{k=1,\ldots,l}{max} KS(I_k) \\ KS(I_k) = \max_y |F_y(y) - F_{y|\tilde{x_i}}(y|\tilde{x_i} \in I_k)| \end{cases} \tag{5}$$

where $\hat{S}_i$ is sensitivity index; KS is Kolmogorov-Smirnov statistic; $F_y(y)$ is unconditional CDF where $y \subseteq Y$ and $F_{y|\tilde{x_i}}(y|\tilde{x_i} \in I_k)$ is conditional CDF where $\tilde{x_i}$ is fixed. Using Eq. (5) to compute the sensitivity index ensures there is no need to specify N_c. It coincides with the number of points in I_k as approximately N/n, where N is the size of the generic sample. As for the unconditional sample N_u, a better option is to use subsample of Y as the conditional ones i.e., $N_u = N_c$.

The process of SA executed by PAWN combined with ML is shown in Algorithm 1. In this algorithm, 'LIBSVM' is used as an SVM tool to train the surrogate model [32]. The model training parameters like 's', 't', 'bestc', 'bestg', 'p', 'v', and the introduction of functions like 'SVMcgForRegress', 'libsvmtrain', and 'libsvmpredict' can be found in [32]. This algorithm mainly includes three parts. The first part is modelling (line 2-6). The thrust of all thrusters is the model input, and the positioning capability as defined by Cri above is the model output. ML is employed to construct a surrogate model between the model input and output. The second part is resampling (line 6-7). 'Unconditional_sampling' is used to generate unconditional samples; 'PAWN_sampling' is used to gain conditional samples. The last part is sensitivity index computation (line 9-10). The 'PAWN' indices of all thrusters are computed by 'PAWN_index'. Its function is shown in line 11-17. Line 12-13 is to calculate the unconditional output and conditional output. Line 14-16 is to compute the 'PAWN' index using Eq. (5). Detailed computing process could be found in [31]. The introduction of parameters and functions regarding PAWN method can be found in [22].

Algorithm 1: SA algorithm

Input: $Thrust$,Cri s, t, p, v
Output: SA_index
1 **for** $i = 1$: num **do**
2 $X \leftarrow Thrust$
3 $Y \leftarrow Cri$
4 $[bestc, bestg] \leftarrow SVMcgForRegress(X, Y)$
5 $cmd \leftarrow [s, t, bestc, bestg, p, v]$
6 $model \leftarrow libsvmtrain(X, Y, cmd)$
7 $U \leftarrow Unconditional\_sampling$
8 $C \leftarrow PAWN\_sampling$
9 $index(i) \leftarrow PAWN\_index(U, C, model)$
10 $SA\_index \leftarrow index/num$
11 **Function** $PAWN\_index(Xu, XX, model)$**:**
12 $Yu \leftarrow libsvmpredict(Xu, model)$
13 $YY \leftarrow libsvmpredict(XX, model)$
14 $[YF, Fu, Fc] \leftarrow PAWN\_cdf(Yu, YY)$
15 $KS \leftarrow PAWN\_ks(YF, Fu, Fc)$
16 $index \leftarrow max(KS)$
17 **return** index

Table 2
Parameters of the offshore vessel.

Items	Values
Length between perpendicilars [m]	82.7
Breadth [m]	23.0
Draught [m]	7.5
Tunnel thruster propulsion [KN]	≤173.0
Main thruster propulsion [KN]	≤1350.0

Table 3
The variables of DP data.

	Inputs	Unit
Ship status	east position	[m]
	west position	[m]
	heading	[deg]
Thruster1	rpm	[RPM]
	thrust	[KN]
	consumed power	[KW]
Thruster2	rpm	[RPM]
	thrust	[KN]
	consumed power	[KW]
Thruster3	rpm	[RPM]
	thrust	[KN]
	consumed power	[KW]
Thruster4	rpm	[RPM]
	thrust	[KN]
	consumed power	[KW]
Thruster5	rpm	[RPM]
	thrust	[KN]
	consumed power	[KW]
Thruster6	rpm	[RPM]
	thrust	[KN]
	consumed power	[KW]

Table 4
Environment and thruster failures setting for significance analysis.

Sea states	Attack angle [deg]	Thruster failure
Strong breeze	45	011111
		101111
		110111
		111011
		111101
		111110
		110110
Strong breeze	90	101111
		110110
Strong breeze	135	101111
		110110
Fresh breeze	45	101111
		110110

4. Case study

4.1. An optimal ML selection based on Ishigami function

In order to find an optimal modeling method, first of all, three prevalent ML methods, such as back propagation (BP), regularized extreme learning machine (RELM), and SVM, are introduced into training models [16, 33, 34]. Next, PAWN combined with these three models is used to compute sensitivity indices of three parameters of Ishigami function. Finally, SA results are compared with a benchmark to identify the optimal ML method for analyzing the significance of thrusters.

In the course of determining an optimal ML method, Ishigami function is selected as a mathematical model, because Ishigami is a widely-used benchmark model that is applied to test the validity of sensitivity analysis method [17]. It is shown in Eq. (6).

$$y = sin(\chi_1) + asin(\chi_2)^2 + b\chi_3^4 sin(\chi_1) \tag{6}$$

where a and b are random constants that can influence the sensitivity index of χ_i, $i \in \{1, 2, 3\}$. χ_i follows a uniform distribution over $[-\pi, \pi]$. Here, we set $a = 2$ and $b = 1$. Fig. 4 displays SA results as well as benchmark value. The dotted line is the benchmark value of sensitivity indices of the three parameters χ_i in Eq. (6). The corresponding sensitivity indices are S_1=0.53, S_2=0.19, and S_3=0.35, respectively. It is evident that both BP and RELM cannot figure sensitivity index out correctly; whereas PAWN combined with SVM has a better approximation to the benchmark. Therefore, SVM is selected as modelling method in the follow-up sensitivity analysis of thrusters in different scenarios.

4.2. Experimental design

This significance analysis of thrusters is conducted to determine the variation of positioning capability apportioned to each thruster. The specifications of the vessel are listed in Table 2. This vessel is actuated by six thrusters shown in Fig. 3. The actuator forces relate to the control forces and moments by $\boldsymbol{\tau} = \boldsymbol{T}(\boldsymbol{\xi})\boldsymbol{f}$, where $\boldsymbol{\xi} = [\xi_1, ..., \xi_p] \in \mathbb{R}^p$ is a vector of azimuth angles and $\boldsymbol{T}(\boldsymbol{\xi})$ is the thrust configuration matrix [35]. In this paper, ξ is fixed. In order to obtain the demanded thrust for each thruster, an unconstrained least-squares (LS) optimization problem is constructed. Through using Lagrange Multipliers to solve LS

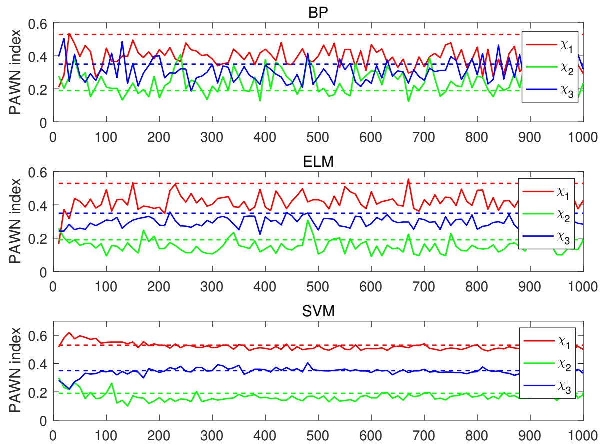

Figure 4: SA results computed by PAWN based on different ML methods.

optimization problem, we can obtain $\boldsymbol{f} = \boldsymbol{T}^{\dagger}\boldsymbol{\tau}$, where $\boldsymbol{T}^{\dagger} = \boldsymbol{W}^{-1}\boldsymbol{T}^{\top}(\boldsymbol{T}\boldsymbol{W}^{-1}\boldsymbol{T}^{\top})^{-1}$ is recognized as the generalised inverse (GI) matrix. Here, $\boldsymbol{W}$ is a positive definite matrix weighting the control forces. The detailed reasoning process has been interpreted in [35].

The attack angles α is set as $[45°, 90°, 135°]$ for different scenarios. The direction of current and wave is fixed for simplifying the experiment. The limits of ship position and heading are set as R = 3m and $\theta = 6°$, respectively. Table 4 lists four different combinations of sea states and attack angle. They are 'strong breeze 45°', 'strong breeze 90°', 'strong breeze 135°', and 'fresh breeze 45°'. For 'strong breeze 45°', there are seven different thruster failure modes represented by binary string: '011111', '101111', '110111', '111011', '111101', '111110','110110'. Here, '0' denotes the thruster is malfunctioning; '1' denotes the thruster is working normally. For example, '101111' indicates the second thruster is malfunctioning while the others are working normally. The required parameters of ship states are listed in the Table 3. The sampling frequency is set as 20HZ.

The synthesized criterion involves specifying three weighting factors: ω_1, ω_2 and ω_3. In this study, we set $\omega_1 = 0.5$, $\omega_2 = 0.4$, and $\omega_3 = 0.1$ based on the following reasons. On the one hand, since DP vessels are designed with the redundant power system, in general, 20% of power will be reserved to avoid loss-of-position occurrence. That indicates the power is sufficient to keep a vessel's position and heading during DP operations. Therefore, power utilization was considered the least important factor in the criterion. On the other hand, ship position is seen as the most significant factor because the loss of position brings a more considerable detrimental impact on DP operations than heading. For PAWN, n is set to 10 based on the samples of data as well as experience as described in other papers [16, 31].

In this paper, the experiment investigates the significance of thrusters under circumstances of different thruster failures in two sea states. Using the proposed method for timely computation of thrusters' sensitivity is studied as well.

4.3. Significance analysis in different thruster failure modes at two sea states

This section mainly analyzes and compares SA results in different environmental factors and thruster conditions. Table 5 lists the SA results of thruster failures at the strong breeze and fresh breeze sea states. It is found that thruster 5 is more significant than the rest of thrusters in most cases. Its contribution accounts for around 30% $\sim$ 40%. Especially, when thruster 6 fails to work, the significance of thruster 5 exceeds 35% because thruster 5 as the only main propeller must generate much more thrust to counteract the influence of environmental disturbances. When one thruster failure occurs, the significance of thrusters that play a complementary role will have a significant increase as shown in Table 5. For example, the PAWN index of thruster 6 increases from 8% to 30% when thruster 5 fails in 'strong breeze 45°'. The same happens to thruster 1 and 2. For the case of '101111' in 'strong breeze 45°', for instance, the significance of thruster 1 rises by 13% up to 26.42%. For dual thruster failure '110110' in all sea states, at least two of tunnel thrusters' significance go up to over 20% compared with one thruster failure. That possibly results from the drastic variation of the ship heading. It is reflected from the above analysis that the significance of thrusters depends on the conjunction of sea states, wind direction as well as thruster failures.

Next, significance analysis of thrusters is carried out in detail from the respect of statistics and SA. In order to illustrate how to do analysis by SA coupled with statistical analysis, we will use '111111' in the case of strong breeze with attack angle 45° as an example. For the case of '111111' in 'strong breeze 45°', an average of thrust and SA results are shown in Fig. 5. The left y-axis represents the PAWN index of each thruster while the right one denotes mean value of thrust. These two analysis methods are able to show the importance of thrusters from their own perspective. In addition, there are interior connections between these two methods. The results of SA show that the order of importance of thrusters is quite as similar as that of statistical analysis. The PAWN index shows that thruster 5 has the most influential effect on positioning capability, at 29.76%. The second-largest effect is thruster 4, accounting for roughly 22.46%. Thrusters 3, 1, 2, and 6 follow in that order. Thruster 6 makes only an 8.17% contribution to the station-keeping ability of DP vessel despite its similarities to thruster 5, which makes the largest contribution. However these two methods show some distinctions, such as inconsistency of SA results with statistical analysis for thruster 6.

From the perspective of statistics, thruster 6 has as much thrust as thruster 5 as shown in Fig. 6. The mean and variance of thrust generated by thruster 5 are the same as those generated by thruster 6. The two thrusters also consume the same amount of power and have similar statistical features. But observing results obtained by the proposed SA method in Fig. 5, in which all SA indices are drawn as blue bars, shows that thruster 6 is far less significant than thruster 5. It

Table 5
SA results of thruster failures in strong breeze and fresh breeze.

Sea states	Direction (deg)	Thruster failure	PAWN index Thr1	Thr2	Thr3	Thr4	Thr5	Thr6
Strong breeze	45	111111	0.1342	0.1040	0.1576	0.2246	**0.2976**	0.0817
		011111	0	**0.3701**	0.1448	0.1480	0.2284	0.1087
		101111	0.2642	0	0.0604	0.1069	**0.3222**	0.2459
		110111	0.1992	0.2080	0	0.0850	**0.3058**	0.2019
		111011	0.1415	0.2483	0.0853	0	**0.3472**	0.1775
		111101	0.2629	0.1839	0.1433	0.1098	0	**0.3000**
		111110	0.1674	0.1225	0.1435	0.1456	**0.4209**	0
		110110	0.2106	0.2026	0	0.2050	**0.3818**	0
	90	111111	**0.2877**	0.1211	0.0829	0.1485	0.1313	0.2283
		101111	0.2723	0	0.1103	0.1100	**0.2985**	0.2089
		110110	0.0737	0.3337	0	0.2392	**0.3534**	0
	135	111111	0.1832	0.1638	0.1224	0.1888	**0.2544**	0.0873
		101111	0.0987	0	**0.3491**	0.3273	0.1268	0.0980
		110110	0.2285	**0.4016**	0	0.0997	0.2702	0
Fresh breeze	45	111111	0.1373	0.0729	0.1317	0.0771	**0.3460**	0.2350
		101111	0.2591	0	0.1007	0.0901	**0.3401**	0.2099
		110110	0.1826	0.2113	0	0.2282	**0.3780**	0

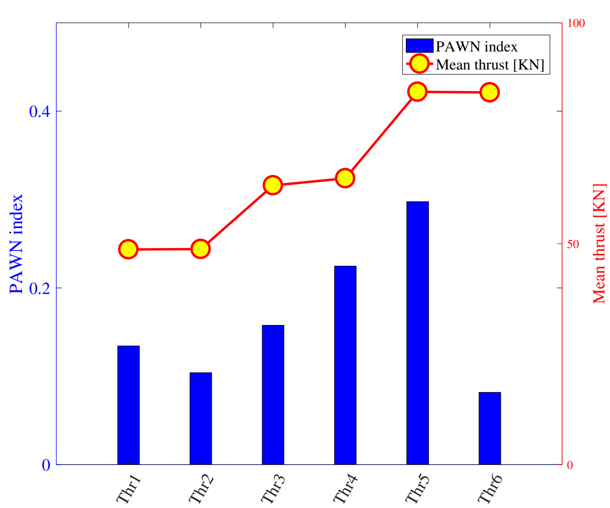

Figure 5: The SA result and average thrust of 6 thrusters for '111111' in 'strong breeze 45°'.

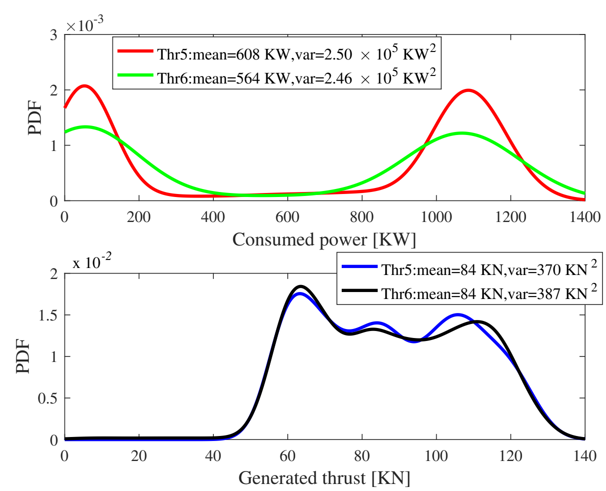

Figure 6: The PDF of consumed power and thrust generated by thrusters 5 and 6 for '111111' with strong breeze and $\alpha = 45°$.

is even less than thruster 2. It reveals that SA results do not entirely conform with results obtained by statistical analysis. Both methods did give us insights that thruster 6 consumed amounts of power but generated too much useless force in this case.

To obtain more insights from Fig. 5, thrusters 4 and 6 are for detailed investigation. Fig. 7 displays the PDF of power consumed by thrusters 4 and 6 respectively. The power consumed mostly appears in the interval [100 KW, 600 KW], which is far less than the power consumed by thruster 6 as shown in the blue area. Moreover, the mean of thrust generated by thruster 4 is far less than that generated by thruster 6. Based on Fig. 5 and Fig. 7, we can find that thruster 6 consumed more power and generated more thrust but less contribution than thruster 4.

Through SA and statistical analysis, it is definitely found that some thrusters have fewer influences on DP capability, although they consumed more power. That results in

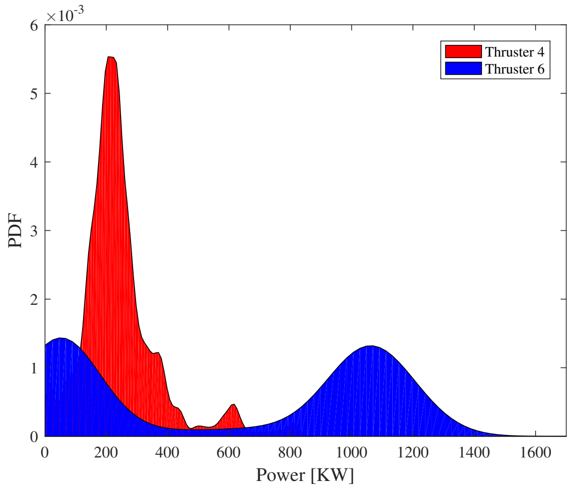

Figure 7: The power consumed by thrusters 4 and 6 in ‘strong breeze 45° 111111’.

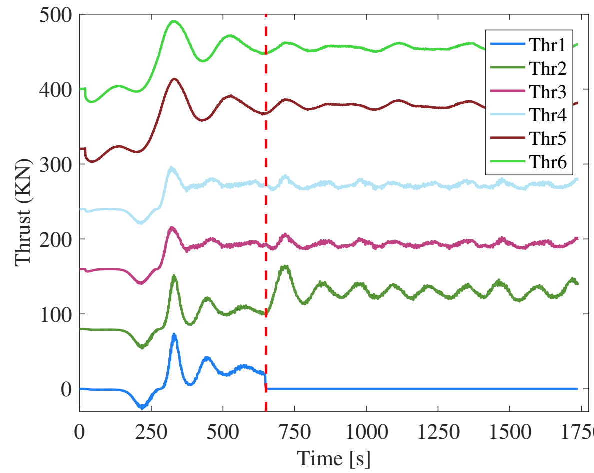

Figure 8: Time-domain variation of thrust from ‘111111’ to ‘011111’.

a waste of power. Therefore, significance results could be used to provide guidance to improve the power allocation algorithm. For example, sensitivity indices as weighting factors are added into the algorithm. In this case, thruster 6 with high power consumption but a little contribution to DP capability will be reallocated less power by the power system. Instead, more power should be redistributed to thruster 4, which could improve DP capability with low power consumption.

4.4. Real-time computation of thrusters’ sensitivity

Although the existing method is efficient to analyze the thrusters’ significance in [11], it is not competent in the real-time computation of thrusters’ sensitivity. This section is to verify the feasibility of the proposed method in estimating thrusters’ sensitivity online.

A simulation experiment is carried out when thruster state changes from ‘111111’ to ‘011111’ in ‘strong breeze 45°’. The thrust generated by thrusters is shown in Fig. 8. Red dotted line represents the point at which thruster 1 fails to work. In order to visualize each curve clearly, multiple shifts of 80 KN along the y-axis direction is performed for thruster 2-6. In fact, the value of the thrust of all thrusters starts from 0.

Fig. 9 shows the variation of sensitivity indices of thrusters over time. The horizontal axis denotes sensitivity index is computed at a window time of 25s that comprises 500 sample points. Evidently, the proposed method is able to gain the contribution of each thruster to the DP capability in the process of vessel counteracting against environmental forces. Especially, when thruster 1 shuts down at 650s depicted by a red circle, the importance of thruster 1 becomes 0 thereafter. On the other hand, thruster 2 plays a more and more important role since this point. This is because thruster 1 and 2 are bow thrusters, as shown in Fig. 3, the malfunction of thruster 1 leads to the rise of thruster 2 importance in the long term. In addition, the importance of other thrusters rises to some extent as well after thruster 1 fails to work.

At the point of 650s, the detailed information can be found in the Fig. 10. From this figure, the importance of thruster 2 and 4 grow rapidly compared with other thrusters. Therefore, the instant change of the indices could provide the operator evidence to improve the power-consuming of thruster 2 and 4 to promote the DP capability quickly after the failure of thruster 1.

To sum up, the proposed method is capable of finding the contribution of all thrusters in a real-time manner.

4.5. Discussion

For the case of ‘111111’ in ‘strong breeze 45°’ in Fig. 6, the discrepancy in terms of power and thrust between thruster 5 and 6 possibly results from the fact that the rudder angle of main thrusters is fixed. As shown in Fig. 3, in order to resist the wind whose attack angle is 45°, thruster 5 must bear much more load than thruster 6. Therefore, the power and thrust of thruster 5 vary more drastically compared with those of thruster 6. It can be shown from the above analysis that thruster’s importance is affected by a synthesized factor, including the configuration of thrusters, the attack angle of sea states, and the thrust allocation algorithm.

In Fig. 4, the result of BP and ELM is not as ideal as that of SVM. This situation mainly results from the limited training sample on account of online significance analysis. Considering the requirement of on-board support, therefore, SVM is used for the real-time estimation of sensitivity indices. Since the sensitivity index computed by SVM can converge to a stable value after 500 training samples, we chose a window time of 25s corresponding to 500 training samples under the sampling frequency of 20HZ in Section 4.4.

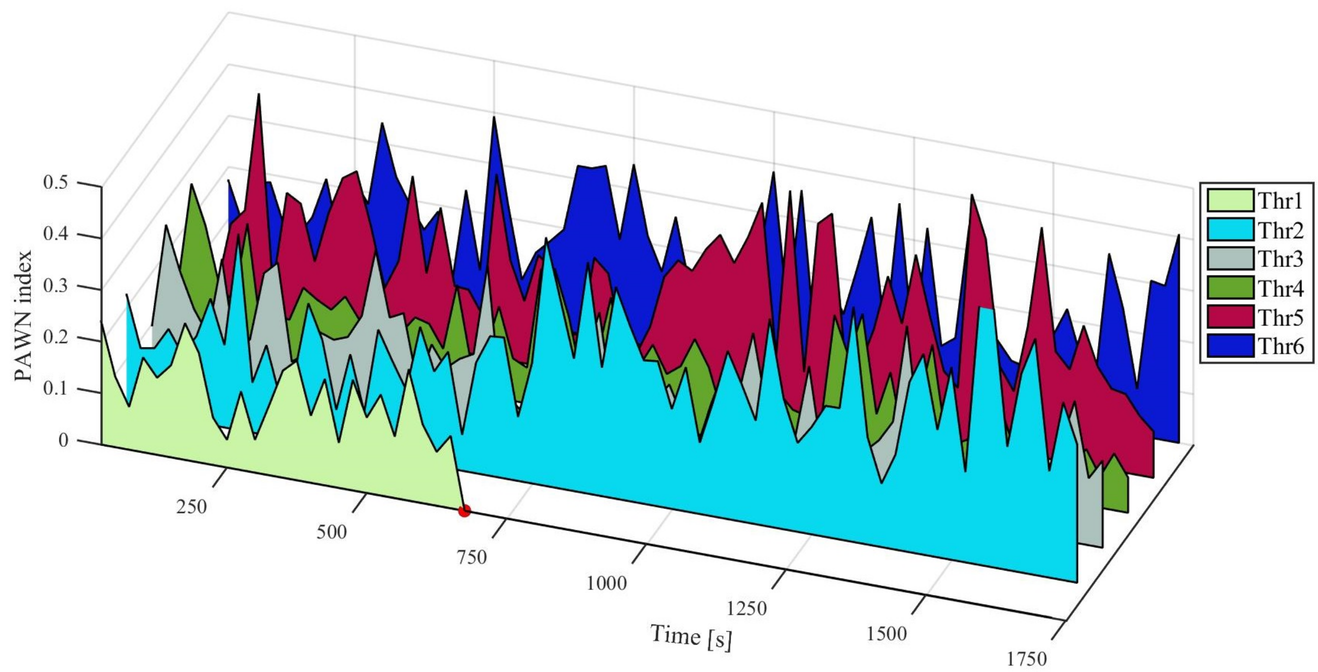

Figure 9: Real-time computation of the significance of thrusters.

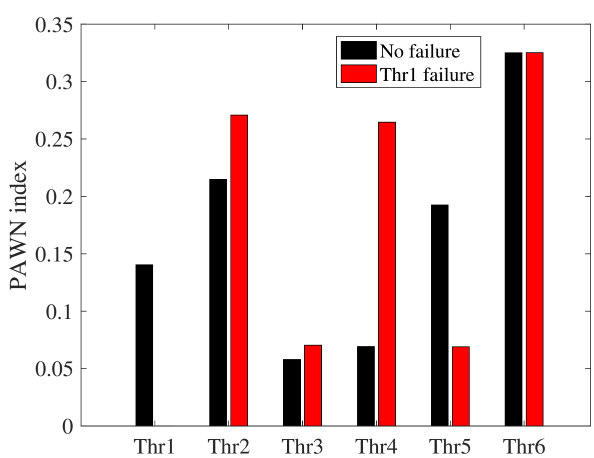

Figure 10: The instant variation of the significance of thrusters before and after thruster 1 failure.

5. Conclusion

This paper proposes a method that mainly focuses on studying the significance of thrusters based on a synthesized positioning capability criterion in different thruster failure conditions. In order to quantify the DP capability, a synthesized assessment criterion is proposed by integrating ship position, heading and power. Next, the Ishigami function is used as a benchmark to determine an optimal modelling method. Through the comparison with ANN and ELM, SVM is selected to construct a surrogate model between thrusters and DP capability. Finally, different thruster failure cases in two sea states are designed to elaborate on how statistical features and SA are combined to quantify and analyze the significance of thrusters.

The purpose of significance analysis results is as follows: 1) they can provide onboard support to control power system to allocate more power to the most significant thruster when thruster fails to work, which contributes to efficiently improving DP capability; 2) they also can be used to provide guidance to optimize power allocation. By observing statistics of power, and sensitivity results, thrusters that consumed more power but made much less contribution to positioning capability should be reallocated less power. This is able to be accomplished by, for example, adding sensitivity indices as weighting factors into the allocation algorithm. That is helpful to improve vessel's DP capability with less power consumption.

For future work, efforts will be put on investigating the impact of azimuth thrusters and the thrust allocation logic on the significance of thrusters in DP operations.

Acknowledgment

The research is supported by a grant from the IKTPLUSS Project "Remote Control Centre for Autonomous Ship Support" (Project nr: 309323), and by a grant from the Research Based Innovation "SFI Marine Operation in Virtual Environment (SFI-MOVE)" (Project nr: 237929) in Norway. The author Chunlin Wang would like to thank the sponsorship of the Chinese Scholarship Council for funding his research at Norwegian University of Science and Technology. The authors would like to thank Offshore Simulator Centre for their support in relation to performing the simulation study.

References

[1] D. AS, Assessment of station keeping capability of dynamic positioning vessels (2016).

[2] D. Lee, S. J. Lee, S. C. Yim, Reinforcement learning-based adaptive pid controller for dps, Ocean Engineering 216 (2020) 108053.

[3] A. H. Brodtkorb, S. A. Værnø, A. R. Teel, A. J. Sørensen, R. Skjetne, Hybrid controller concept for dynamic positioning of marine vessels with experimental results, Automatica 93 (2018) 489–497.

[4] P. Han, G. Li, R. Skulstad, S. Skjong, H. Zhang, A deep learning approach to detect and isolate thruster failures for dynamically positioned vessels using motion data, IEEE Transactions on Instrumentation and Measurement (2020).

[5] R. Skulstad, G. Li, T. I. Fossen, B. Vik, H. Zhang, Dead reckoning of dynamically positioned ships: Using an efficient recurrent neural network, IEEE Robotics & Automation Magazine 26 (3) (2019) 39–51.

[6] H. Chen, B. Nygärd, et al., Quantified risk analysis of dp operations-principles and challenges, in: SPE International Conference and Exhibition on Health, Safety, Security, Environment, and Social Responsibility, Society of Petroleum Engineers, 2016.

[7] A. Karlsen, L. Pivano, E. Ruth, Dnv gl dp capability-a new standard for assessment of the station-keeping capability of dp vessels, in: proceedings of Marine Technology Society (MTS) DP Conference, Houston (TX), USA, 2016, pp. 1–15.

[8] S. Xu, X. Wang, L. Wang, X. Li, Investigation of the positioning performances for dp vessels considering thruster failure modes by a novel synthesized criterion, Journal of Marine Science and Technology (2017) 1–15.

[9] F. Benetazzo, G. Ippoliti, S. Longhi, P. Raspa, Advanced control for fault-tolerant dynamic positioning of an offshore supply vessel, Ocean Engineering 106 (2015) 472–484.

[10] X. U. Sheng wen, X. F. Wang, L. Wang, A dynamic positioning capability analysis for a semi-submersible considering thruster failure mode, Journal of Ship Mechanics (2016).

[11] S. Xu, X. Wang, L. Wang, S. Meng, B. Li, A thrust sensitivity analysis based on a synthesized positioning capability criterion in dpcap/dyncap analysis for marine vessels, Ocean Engineering 108 (2015) 164–172.

[12] X. Cheng, G. Li, R. Skulstad, S. Chen, H. P. Hildre, H. Zhang, A neural-network-based sensitivity analysis approach for data-driven modeling of ship motion, IEEE Journal of Oceanic Engineering 45 (2) (2019) 451–461.

[13] L. Pivano, D. Nguyen, Ø. Smøgeli, Full-scale validation of a vessel's station-keeping capability with dyncap, in: ASME 2017 36th International Conference on Ocean, Offshore and Arctic Engineering, American Society of Mechanical Engineers, 2017, pp. V009T12A054–V009T12A054.

[14] L. Wang, J.-m. Yang, S.-w. Xu, Dynamic positioning capability analysis for marine vessels based on a dpcap polar plot program, China Ocean Engineering 32 (1) (2018) 90–98.

[15] L. Pivano, Ø. Smøgeli, S. Muddusetti, J. Ramsey, Better analysis-better data-better decisions-better operational risk management= delivery of incident free operations: Enabled by dyncap, in: Dyn. Position. Conf, 2014.

[16] C. Wang, X. Cheng, S. Chen, G. Li, H. Zhang, A svm-based sensitivity analysis approach for data-driven modeling of ship motion, in: 2018 IEEE International Conference on Mechatronics and Automation (ICMA), IEEE, 2018, pp. 803–808.

[17] F. Pianosi, T. Wagener, A simple and efficient method for global sensitivity analysis based oncumulative distribution functions, Environmental Modelling and Software 67 (2015) 1–11.

[18] V. Todorov, I. Dimov, T. Ostromsky, S. Apostolov, R. Georgieva, Y. Dimitrov, Z. Zlatev, Advanced stochastic approaches for sobol'sensitivity indices evaluation, Neural Computing and Applications (2020) 1–16.

[19] S. Tarantola, T. A. Mara, Variance-based sensitivity indices of computer models with dependent inputs: The fourier amplitude sensitivity test, International Journal for Uncertainty Quantification 7 (6) (2017).

[20] I. Kovacs, A. Iosub, M. Ţopa, A. Buzo, G. Pelz, A gradient-based sensitivity analysis method for complex systems, in: 2019 IEEE 25th International Symposium for Design and Technology in Electronic Packaging (SIITME), IEEE, 2019, pp. 333–338.

[21] F. K. Zadeh, J. Nossent, F. Sarrazin, F. Pianosi, A. V. Griensven, T. Wagener, W. Bauwens, Comparison of variance-based and moment-independent global sensitivity analysis approaches by application to the swat model, Environmental Modelling & Software 91 (C) (2017) 210–222.

[22] F. Pianosi, F. Sarrazin, T. Wagener, A MATLAB toolbox for global sensitivity analysis, Elsevier Science Publishers B. V., 2015.

[23] W. Yun, Z. Lu, X. Jiang, An efficient method for moment-independent global sensitivity analysis by dimensional reduction technique and principle of maximum entropy, Reliability Engineering & System Safety 187 (2019) 174–182.

[24] E. Plischkeabc, Global sensitivity measures from given data, European Journal of Operational Research 226 (3) (2013) 536–550.

[25] G. Li, B. Kawan, H. Wang, H. Zhang, Neural-network-based modelling and analysis for time series prediction of ship motion, Ship technology research 64 (1) (2017) 30–39.

[26] W. Zhang, Z. Liu, Real-time ship motion prediction based on time delay wavelet neural network, Journal of Applied Mathematics 2014 (2014).

[27] P. Mizythras, E. Boulougouris, A. Priftis, A. Incecik, O. Turan, D. Reddy, Sensitivity analysis of the tool for assessing safe manoeuvrability of ships in adverse sea conditions, in: International Conference on Shipping in Changing Climates 2016, 2016, pp. 1–13.

[28] M. Schneider, W. Ertel, F. Ramos, Expected similarity estimation for large-scale batch and streaming anomaly detection, Machine Learning 105 (3) (2016) 1–29.

[29] F. T. Liu, K. M. Ting, Z. H. Zhou, Isolation-based anomaly detection, Acm Transactions on Knowledge Discovery from Data 6 (1) (2012) 1–39.

[30] S. Kuhlmann, M. Tressl, Comparison of exponential-logarithmic and logarithmic-exponential series, Mathematical Logic Quarterly 58 (6) (2012) 434–448.

[31] F. Pianosi, T. Wagener, Distribution-based sensitivity analysis from a generic input-output sample, Environmental modelling & software 108 (2018) 197–207.

[32] C.-C. Chang, C.-J. Lin, LIBSVM: A library for support vector machines, ACM Transactions on Intelligent Systems and Technology 2 (2011) 27:1–27:27, software available at `http://www.csie.ntu.edu.tw/~cjlin/libsvm`.

[33] K. Cui, X. Jing, Research on prediction model of geotechnical parameters based on bp neural network, Neural Computing and Applications 31 (12) (2019) 8205–8215.

[34] Z. Shao, M. J. Er, An online sequential learning algorithm for regularized extreme learning machine, Neurocomputing 173 (2016) 778–788.

[35] T. I. Fossen, Handbook of marine craft hydrodynamics and motion control, John Wiley & Sons, 2011.